Front. Phys. China, 2008, 3(2): 195–204
DOI 10.1007/s11467-008-0017-z

REVIEW ARTICLE

Zeraoulia ELHADJ, J. C. SPROTT

On the robustness of chaos in dynamical systems: Theories and applications

Abstract This paper offers an overview of some important issues concerning the robustness of chaos in dynamical systems and their applications to the real world.

Keywords robust chaos, theories, methods, real applications

PACS numbers 05.45.-a, 05.45.Gg

1 Introduction

Chaotic dynamical systems display two kinds of chaotic attractors: One type has fragile chaos (the attractors disappear with perturbations of a parameter or coexist with other attractors), and the other type has robust chaos, defined by the absence of periodic windows and coexisting attractors in some neighborhood of the parameter space. The existence of these windows in some chaotic regions means that small changes of the parameters would destroy the chaos, implying the fragility of this type of chaos.

Contrary to this situation, there are many practical applications, such as in communication and spreading the spectrum of switch-mode power supplies to avoid electromagnetic interference [15, 16], where it is necessary to obtain reliable operation in the chaotic mode, and thus robust chaos is required. Another practical example can be found in electrical engineering where robust chaos is demonstrated in Ref. [13]. The occurrence of robust chaos in a smooth system is proved and discussed in Ref. [2], which includes a general theorem and a practical procedure for constructing S-unimodal maps that generate robust chaos. This result contradicts the conjecture that robust chaos cannot exist in smooth systems [13]. On the other hand, there are many methods used to search for a smooth and robust chaotic map, for example in Refs. [1−5], where a one-dimensional smooth map that generates robust chaos in a large domain of the parameter space is presented. In Ref. [6], simple polynomial unimodal maps that show robust chaos are constructed. Other methods and algorithms are given in the discussion below.

This paper is organized as follows. In the following section, we first discuss robust chaos, its theories and applications, and then give in Section 3 several rigorous, numeric, and experimental results that explain the different methods for the generation of robust chaos in dynamical systems. The final section concludes the paper.

Zeraoulia ELHADJ[1], J. C. SPROTT[2]

[1] Department of Mathematics, University of Tébéssa, 12000, Algeria
[2] Department of Physics, University of Wisconsin, Madison, WI 53706, USA
E-mail: zeraoulia@mail.univ-tebessa.dz, zelhadj12@yahoo.fr; sprott@physics.wisc.edu

Received January 12, 2008; accepted February 20, 2008

2 Why robust chaos?

The past decade has seen heightened interest in the exploitation of robust chaos for applications to engineering systems. Since there are many areas for applications of robust chaos, we concentrate on two examples of applications of robust chaos in the real world. The first is given in Ref. [41], which suggests a new approach (with experiments, statistical analysis, and key space

analysis) for image encryption based on a robust high-dimensional chaotic map. The new scheme employs the so-called cat map to shuffle the positions and then confuses the relationship between the cipher-image and the plain-image by using the high-dimensional preprocessed Lorenz chaotic map. This work shows that the proposed image encryption scheme provides an efficient and secure means for real-time image encryption and transmission. The second example is given in Ref. [54], which uses the notion of robust chaos in another new encryption scheme. A recent bibliography on the applications of robust chaos in the real world are collected in these papers [11, 13, 15, 16, 21, 30, 41−43, 48−51, 58, 60−66, 77−80].

3 Theories and applications of robust chaos

3.1 Robust chaos in 1-D maps

In this section, we give several methods to generate robust chaos in 1-D (one-dimensional) maps.

3.1.1 Robust chaos in 1-D piecewise-smooth maps

As an example of the occurrence of robust chaos in 1-D piecewise-smooth maps, the following model of networks of neurons with the activation function $f(x) = |\tanh s(x-c)|$ is studied in Ref. [43], where it was shown that in a certain range of s and c the dynamical system

$$x_{k+1} = |\tanh s(x_k - c)| \tag{1}$$

cannot have stable periodic solutions, which proves the robustness of chaos.

3.1.2 Robust chaos in 1-D smooth maps

The robustness of chaos in the sense of the above definition is expected to be relevant for any practical applications of chaos, and it was shown to exist in a general family of piecewise-smooth two-dimensional maps, but was conjectured to be impossible for smooth unimodal maps [8−13]. However, it is shown in Ref. [1, 2], respectively, that the following 1-D maps have robust chaotic attractors:

$$f(x,\alpha) = \frac{1 - x^{\alpha} - (1-x)^{\alpha}}{1 - 2^{1-\alpha}}$$

$$f(\phi(x), v) = \frac{1 - v^{\pm\phi(x)}}{1 - v^{\pm\phi(c)}} \tag{2}$$

where α, v are bifurcation parameters and $\phi(x)$ is unimodal with a negative Schwarzian derivative (but not necessarily chaotic), and c is the critical point of $\phi(x)$, i.e. $\dot{\phi}(c) = 0$.

Also in Ref. [5], the following map is shown to be robust:

$$f_{m,n}(x,a) = 1 - 2(ax^m + bx^n) \tag{3}$$

where $0 \leqslant a \leqslant 1, b = 1-a$, and m, n are even and > 0. On the other hand, it is known that a map $\varphi : I \longrightarrow I$ is S-unimodal on the interval $I = [a, b]$ if: (a) The function $\varphi(x)$ is of class C^3, (b) the point a is a fixed point with b its other preimage, i.e. $\varphi(a) = \varphi(b) = a$, (c) there is a unique maximum at $c \in (a, b)$ such that $\varphi(x)$ is strictly increasing on $x \in [a, c)$ and strictly decreasing on $x \in (c, b]$, and (d) φ has a negative Schwarzian derivative, i.e.,

$$S(\varphi, x) = \frac{\varphi'''(x)}{\varphi'(x)} - \frac{3}{2}\left[\frac{\varphi''(x)}{\varphi'(x)}\right]^2 < 0 \tag{4}$$

for all $x \in I - \{y, \varphi'(y) = 0\}$. Since what matters is only its sign, one may as well work with the product:

$$\hat{S}(\varphi, x) = 2\varphi'(x)\varphi'''(x) - 3[\varphi''(x)]^2 \tag{5}$$

which has the same sign as $S(\varphi, x)$.

The importance of S-unimodal maps in chaos theory comes from the theorem given in Ref. [7] that each attracting periodic orbit attracts at least one critical point or boundary point. Thus, as a result, an S-unimodal map can have at most one periodic attractor which will attract the critical point. This result is used to formulate the following theorem with its proof given in Ref.[2]:

Theorem 1 *Let $\varphi_v(x)$: $I = [a; b] \longrightarrow I$ be a parametric S-unimodal map with the unique maximum at $c \in (a; b)$ and $\varphi_v(c) = b$, $\forall\ v \in (v_{\min}, v_{\max})$, then $\varphi_v(x)$ generates robust chaos for $v \in (v_{\min}, v_{\max})$.*

This theorem gives the general conditions for the occurrence of robust chaos in S-unimodal maps, but it does not give any procedure for the construction of the S-unimodal map $\varphi_v(x)$. A procedure for constructing S-unimodal maps that generate robust chaos from the composition of two S-unimodal maps is given in [2, 4–6].

A 1-D generalization of the well known logistic map [7] is proposed and studied in Ref. [53]. The generalized map is referred to as the β-exponential map, and it is given by

$$GL(\beta, x) = \frac{\beta - x\beta^x - (1-x)\beta^{1-x}}{\beta - \sqrt{\beta}}, 0 \leqslant x \leqslant 1, \beta \geqslant 0 \tag{6}$$

where β is the adjustable parameter. It was proved that the map (6) exhibits robust chaos for all real values of

the parameter $\beta \geqslant e^{-4}$.

Another example of robust chaos is found in Ref. [21], where the robust chaos was identified in a family of discounted dynamic optimization problems in economics (with verification of some properties such as monotonicity and concavity of the return functions and the aggregative production function) in which the immediate return function depends on current consumption, capital input, and a taste parameter. It was shown also that the optimal transition functions are represented by the quadratic family, well-studied in the literature on chaotic dynamical systems.

An hierarchy of many-parameter families of maps on the interval [0,1] having an analytic formula of the Kolmogorov–Sinai entropy was introduced in Ref. [6]. These types of maps do not have period-doubling or period-$n$tupling cascade bifurcations to chaos, but they have single fixed-point attractors in certain regions of parameters space where they bifurcate directly to chaos at exact values of the parameters without the period-n tupling scenario.

3.1.3 Robust chaos in 1-D singular maps

These types of 1-D singular maps play a key role in the theory of up-embedability of graphs [76]. In Ref. [70], the critical behavior of the Lyapunov exponent of a 1-D singular map (which has only one face on a surface) near the transition to robust chaos via type-III intermittency was determined for a family of one-dimensional singular maps. The calculation of critical boundaries separating the region of robust chaos from the region of stable fixed points was given and discussed.

3.2 Robust chaos in 2-D piecewise smooth maps

Power electronics is an area with wide practical application [11–14, 40, 47, 77]. It is concerned with the problem of the efficient conversion of electrical power from one form to another.

Power converters [40, 77] exhibit several nonlinear phenomena such as border-collision bifurcations, coexisting attractors (alternative stable operating modes or fragile chaos), and chaos (apparently random behavior). These phenomena are created by switching elements [40]. Recently, several researchers have studied border-collision bifurcations in piecewise-smooth systems [11–14, 40, 47, 77]. Piecewise-smooth systems can exhibit classical smooth bifurcations, but if the bifurcation occurs when the fixed point is on the border, there is a discontinuous change in the elements of the Jacobian matrix as the bifurcation parameter is varied. A variety of such border-collision bifurcations have been reported in this situation [11, 12, 14]. In Refs. [13, 77] and under certain conditions, border-collision bifurcations produce robust chaos.

Let us consider the following 2-D piecewise smooth system given by

$$g(x,y;\rho)=\begin{pmatrix} g_1=\begin{pmatrix} f_1(x,y;\rho) \\ f_2(x,y;\rho) \end{pmatrix}, & \text{if } x<S(y,\rho) \\ g_2=\begin{pmatrix} f_1(x,y;\rho) \\ f_2(x,y;\rho) \end{pmatrix}, & \text{if } x\geqslant S(y,\rho) \end{pmatrix} \tag{7}$$

where the smooth curve $x = S(y,\rho)$ divides the phase plane into two regions R_1 and R_2, given by

$$R_1=\{(x,y)\in\mathbb{R}^2, x<S(y,\rho)\} \tag{8}$$

$$R_2=\{(x,y)\in\mathbb{R}^2, x\geqslant S(y,\rho)\} \tag{9}$$

It is assumed that the functions g_1 and g_2 are both continuous and have continuous derivatives. Then the map g is continuous, but its derivative is discontinuous at the borderline $x = S(y,\rho)$. It is further assumed that the one-sided partial derivatives at the border are finite and in each subregion R_1 and R_2, the map (7) has one fixed point P_1 and P_2, respectively, for a value ρ_* of the parameter ρ. There are six types of fixed points for the linearized system of the map (7) when the determinant of the Jacobian matrix is positive. The following result is proved in Ref.[14]:

Theorem 2 *When the eigenvalues at both sides of the border are real, if an attracting orbit exists, it is unique (i.e., coexisting attractors cannot occur).*

It is shown in Ref. [12] that the normal form of the map (7) is given by

$$N(x,y)=\begin{cases} \begin{pmatrix} \tau_1 & 1 \\ -\delta_1 & 0 \end{pmatrix}\begin{pmatrix} x \\ y \end{pmatrix}+\begin{pmatrix} 1 \\ 0 \end{pmatrix}\mu, & \text{if } x<0 \\ \begin{pmatrix} \tau_2 & 1 \\ -\delta_2 & 0 \end{pmatrix}\begin{pmatrix} x \\ y \end{pmatrix}+\begin{pmatrix} 1 \\ 0 \end{pmatrix}\mu, & \text{if } x>0 \end{cases} \tag{10}$$

where μ is a parameter and $\tau_i, \delta_i, i = 1,2$ are the traces and determinants of the corresponding matrices of the linearized map in the two subregions R_1 and R_2 evaluated at P_1 (with eigenvalues $\lambda_{1,2}$) and P_2 (with eigenvalues $\omega_{1,2}$), respectively. Now it is shown in Refs. [13, 77] that the resulting chaos from the 2-D map (7) is robust in the following cases:

3.2.1 Case 1

$$\begin{cases} \tau_1 > 1+\delta_1, \text{and } \tau_2 < -(1+\delta_2) \\ 0 < \delta_1 < 1, \text{and } 0 < \delta_2 < 1 \end{cases} \tag{11}$$

where the parameter range for boundary crisis is given by:

$$\delta_1\tau_1\lambda_1 - \delta_1\lambda_1\lambda_2 + \delta_2\lambda_2 - \delta_1\tau_2 + \delta_1\tau_1 - \delta_1^2 - \lambda_1\delta_1 > 0 \tag{12}$$

where the inequality (12) determines the condition for stability of the chaotic attractor. The robust chaotic orbit continues to exist as τ_1 is reduced below $1+\delta_1$.

3.2.2 Case 2

$$\begin{cases} \tau_1 > 1+\delta_1, \text{ and } \tau_2 < -(1+\delta_2) \\ \delta_1 < 0, \text{ and } -1 < \delta_2 < 0 \\ \dfrac{\lambda_1 - 1}{\tau_1 - 1 - \delta_1} > \dfrac{\omega_2 - 1}{\tau_2 - 1 - \delta_2} \end{cases} \tag{13}$$

The condition for stability of the chaotic attractor is also determined by (12). However, if the third condition of (13) is not satisfied, then the condition for the existence of the chaotic attractor changes to

$$\frac{\omega_2 - 1}{\tau_2 - 1 - \delta_1} < \frac{(\tau_1 - \delta_1 - \lambda_2)}{(\tau_1 - 1 - \delta_1)(\lambda_2 - \tau_2)} \tag{14}$$

3.2.3 Case 3

The remaining ranges for the quantity $\tau_i, \delta_i, i = 1, 2$, can be determined in some cases using the same logic as in the above two cases, or there is no analytic condition for a boundary crisis, and it has to be determined numerically.

3.2.4 Example

Several examples of robust chaos in 2-D piecewise smooth systems can be found in [11–14, 40, 47]. In this overview, we give the following example [69].

Consider the unified piecewise-smooth chaotic mapping that contains the Hénon [10] and the Lozi [9] systems defined by

$$U(x,y) = \begin{pmatrix} 1 - 1.4 f_\alpha(x) + y \\ 0.3x \end{pmatrix} \tag{15}$$

where $0 \leqslant \alpha \leqslant 1$ is the bifurcation parameter and the function f_α is given by

$$f_\alpha(x) = \alpha|x| + (1-\alpha)x^2 \tag{16}$$

It is easy to see that for $\alpha = 0$, one has the original Hénon map, and for $\alpha = 1$, one has the original Lozi map, and for $0 < \alpha < 1$, the unified chaotic map (15) is chaotic with different kinds of attractors. In this case it was shown rigorously that the unified system (15) has robust chaotic attractors for $0.493\ 122\ 734 \leqslant \alpha < 1$ as shown in Fig. 1. Some corresponding robust chaotic attractors are shown in Fig. 2. These chaotic attractors cannot be destroyed by small changes in the parameters since small changes in the parameters can only cause small changes in the Lyapunov exponents. Hence the range for the parameter $0 \leqslant \alpha < 1$, in which the map (15) converges to a robust chaotic attractor, is approximately 50.688 percent. This result was also verified numerically by computing Lyapunov exponents and bifurcation diagrams as shown in Fig. 1(a) and (b). For $\alpha < 0.493\ 122\ 734$, the chaos is not robust in some ranges of the variable α because there are numerous small periodic windows as shown in Fig. 3(b) such as the period-8 window at $\alpha = 0.025$. Also, for $\alpha = 0.114$, there are some periodic windows. We note also the existence of some regions in α where the largest Lyapunov exponent is positive, but this does not guarantee the unicity of the attractor, contrary to the case of $\alpha \in [0.493\ 122\ 734, 1]$ where the attractor is guaranteed to be unique due to the analytical expressions.

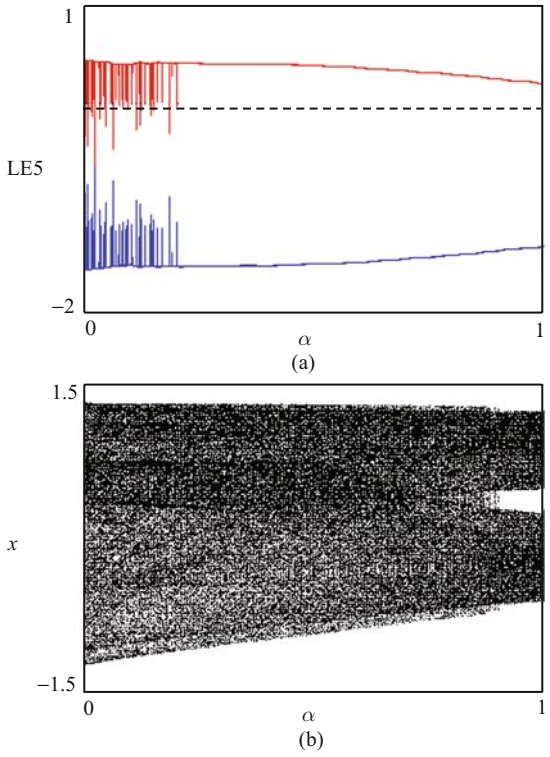

Fig. 1 **(a)** Variation of the Lyapunov exponents of the unified map (15) for $0 \leqslant \alpha \leqslant 1$. **(b)** Bifurcation diagram for the unified chaotic map (15) for $0 \leqslant \alpha \leqslant 1$.

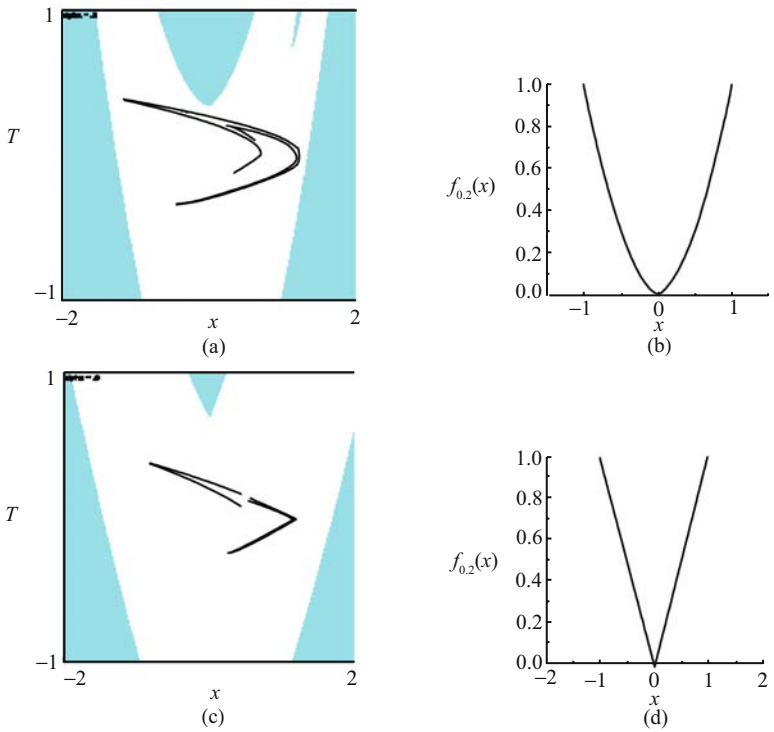

Fig. 2 **(a)** The transition Hénon-like chaotic attractor obtained for the unified chaotic map (15) with its basin of attraction (white) for $\alpha = 0.2$. **(b)** Graph of the function $f_{0.2}$. **(c)** The transition Lozi-like chaotic attractor obtained for the unified chaotic map (15) with its basin of attraction (white) for $\alpha = 0.8$. **(d)** Graph of the function $f_{0.8}$.

3.3 Robust chaos in non-smooth maps

An example of robust chaos in non-smooth maps occurs with the perceptron [24], which is the simplest kind of feedforward neural network and is calculated as

$$f(x) = \begin{cases} 1, \text{ if } \omega \cdot x + b > 0 \\ 0, \text{ else} \end{cases} \tag{17}$$

where ω is a vector of real-valued weights, $\omega \cdot x$ is the dot product (which computes a weighted sum), b is the bias, and a is a constant term that does not depend on any input value. The value of $f(x)$ (0 or 1) is used to classify x as either positive or negative in the case of a binary classification problem. The properties of the time series generated by a perceptron with monotonic and non-monotonic transfer functions were examined in Ref. [71]. The results show that a perceptron with a monotonic function can produce fragile chaos only, whereas a non-monotonic function can generate robust chaos.

3.4 Robust chaos in smooth continuous-time systems

Strange attractors can be classified into three principal classes [39, 44, 52]: hyperbolic, Lorenz-type, and quasi-attractors. The hyperbolic attractors are the limit sets for which Smale's "axiom A" is satisfied and are

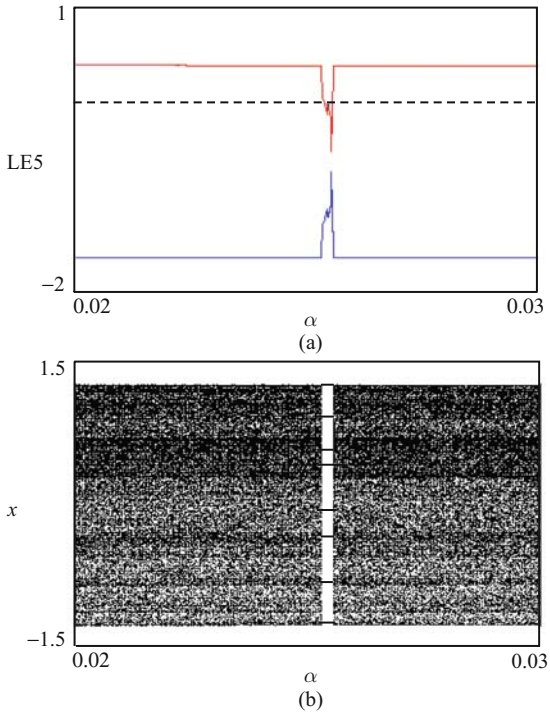

Fig. 3 **(a)** Variation of the Lyapunov exponents for the unified chaotic map (15) for $0.02 \leqslant \alpha \leqslant 0.03$. **(b)** Bifurcation diagram for the unified chaotic map (15) for $0.02 \leqslant \alpha \leqslant 0.03$ showing a period-8 attractor obtained for $\alpha = 0.025$.

structurally stable. Periodic orbits and homoclinic orbits are dense and are of the same saddle type, which is to say that they have the same index (the same dimension for their stable and unstable manifolds). However, the Lorenz-type attractors are not structurally stable, although their homoclinic and heteroclinic orbits are structurally stable (hyperbolic), and no stable periodic orbits appear under small parameter variations, as for example in the Lorenz system [17]. The quasi-attractors are the limit sets enclosing periodic orbits of different topological types (for example stable and saddle periodic orbits) and structurally unstable orbits. For example, the attractors generated by Chua's circuit [45] associated with saddle-focus homoclinic loops are quasi-attractors. Note that this type is more complex than the above two attractors, and thus are not suitable for potential applications of chaos such as secure communications and signal masking. For further information about these types of chaotic attractors, see Ref. [39].

3.4.1 Robust chaos in hyperbolic systems

In strange attractors of the hyperbolic type, all orbits in phase space are of the saddle type, and the invariant sets of trajectories approach the original one in forward or backward time, i.e., the stable and unstable manifolds intersect transversally. Generally, most known physical systems do not belong to the class of systems with hyperbolic attractors [39]. The type of chaos in them is characterized by chaotic trajectories and a set of stable orbits of large periods, not observable in computations because of extremely narrow domains of attraction.

Hyperbolic strange attractors are robust (structurally stable) [44]. Thus, both from the point of view of fundamental studies and of applications, it would be interesting to find physical examples of hyperbolic chaos. For example, the Smale-Williams attractor [46] is constructed for a three-dimensional map, and the composed equations given by

$$\begin{cases} \dot{x} = -2\pi u + (h_1 + A_1 \cos 2\pi\tau/N)\, x - \dfrac{1}{3}x^3 \\ \dot{u} = 2\pi\,(x + \varepsilon_2 y \cos 2\pi\tau) \\ \dot{y} = -4\pi v + (h_2 - A_2 \cos 2\pi\tau/N)\, y - \dfrac{1}{3}y^3 \\ \dot{v} = 4\pi\left(y + \varepsilon_1 x^2\right) \end{cases} \tag{18}$$

are obtained by applying the so-called equations of Kirchhoff [23], where the variables x and u are normalized voltages and currents in the LC circuit of the first self-oscillator (U_1 and I_1, respectively), and y and v are normalized voltages and currents in the second oscillator (U_2 and I_2). Time is normalized to the period of oscillations of the first LC oscillator, and the parameters A_1 and A_2 determine the amplitude of the slow modulation of the parameter responsible for the Andronov-Hopf bifurcation in both self-oscillators. The parameters h_1 and h_2 determine a map of the mean value of this parameter from the bifurcation threshold, and ε_1 and ε_2 are coupling parameters.

The system (18) has been constructed as a laboratory device [46], and an experimental and numerical solution were found. This example of a physical system with hyperbolic chaotic attractor is of considerable significance since it opens the possibility for real applications. For further details, see Ref. [46].

3.4.2 Robust chaos in the Lorenz-type system

As a Lorenz-type system, consider the original Lorenz system [17] given by

$$\begin{cases} \dot{x} = \sigma\,(y - x) \\ \dot{y} = rx - y - xz \\ \dot{z} = -bz + xy \end{cases} \tag{19}$$

These equations have proved to be very resistant to rigorous analysis and also present obstacles to numerical study. A very successful approach was taken in [27, 72] where they constructed so-called geometric models (these models are flows in three dimensions) for the behavior observed by Lorenz for which one can rigorously prove the existence of a robust attractor. Another approach through rigorous numerics [28, 73–75] showed that the equations exhibit a suspended Smale horseshoe. In particular, they have infinitely many closed solutions. A computer-assisted proof of chaos for the Lorenz equations is given in [18–20, 25, 29, 35].

In Ref. [18], a rigorous proof was provided that the geometric model does indeed give an accurate description of the dynamics of the Lorenz equations, i.e., it supports a strange attractor as conjectured by Lorenz in 1963. This conjecture was listed by Steven Smale as one of several challenging mathematical problems for the 21st century [34]. Also, a proof that the attractor is robust, i.e., it persists under small perturbations of the coefficients in the underlying differential equations was given. This proof is based on a combination of normal form theory and rigorous numerical computations. The robust chaotic Lorenz attractor is shown in Fig. 4. As a general result, it was proved in Ref. [38] that the so-called singular-hyperbolic (or Lorenz-like) attractor of a 3-D flow is chaotic in two different strong senses: First, the flow is expansive: if two points remain close for all times, possibly with time reparametrization, then

their orbits coincide. Second, there exists a physical (or Sinai-Ruelle-Bowen) measure supported on the attractor whose ergodic basin covers a full Lebesgue (volume) measure subset of the topological basin of attraction. In particular, these results show that both the flow defined by the Lorenz equations and the geometric Lorenz flows are expansive.

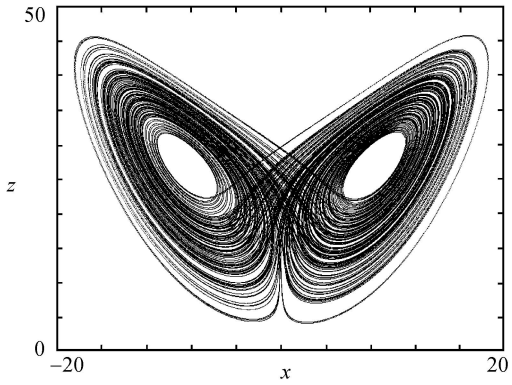

Fig. 4 The robust Lorenz chaotic attractor obtained from (19) for $\sigma = 10, r = 28, b = \dfrac{8}{3}$ [17].

Another proof of the robustness of the Lorenz attractor is given in Ref. [20] where the chaotic attractors of the Lorenz system associated with $r = 28$ and $r = 60$ were characterized in terms of their unstable periodic orbits and eigenvalues. While the Hausdorff dimension is approximated with very good accuracy in both cases, the topological entropy was computed in an exact sense only for $r = 28$. A general method for proving the robustness of chaos in a set of systems called C^1-robust transitive sets with singularities for flows on closed 3-manifolds is given in Ref. [22]. The elements of the set C^1 are partially hyperbolic with a volume-expanding central direction and are either attractors or repellers. In particular, any C^1-robust attractor with singularities for flows on closed 3-manifolds always have an invariant foliation whose leaves are forward contracted by the flow and has a positive Lyapunov exponent at every orbit, showing that any C^1-robust attractor resembles a geometric Lorenz attractor. A new topological invariant (Lorenz-manuscript) leading to the existence of an uncountable set of topologically various attractors is proposed in Ref. [57] where a new definition of the hyperbolic properties of the Lorenz system close to singular hyperbolicity is introduced, as well as a proof that small non-autonomous perturbations do not lead to the appearance of stable solutions.

Other than the Lorenz attractor, there are some works that focus on the proof of the robustness of chaos in 3-D continuous systems, for example the set C^1 introduced in Ref. [22], and a characterization of maximal transitive sets with singularities for generic C^1-vector fields on closed 3-manifolds in terms of homoclinic classes associated with a unique singularity is given and applied to some special cases.

3.4.3 No robust chaos in quasi-attractor-type systems

The complexity of quasi-attractors is essentially due to the existence of structurally unstable homoclinic orbits in the system itself, and in any system close to it. It results in a sensitivity of the attractor structure to small variations of the parameters of the generating dynamical equation, i.e., quasi-attractors are structurally unstable. Then this type of system cannot generate robust chaotic attractors in the sense of this paper [44]. Attractors generated by Chua's circuits [45], given by

$$\begin{cases} \dot{x} = \alpha\,(y - h\,(x)) \\ \dot{y} = x - y + z \\ \dot{z} = -\beta y \end{cases} \tag{20}$$

where

$$h(x) = m_1 x + \tfrac{1}{2}(m_0 - m_1)\,(|x+1| - |x-1|) \tag{21}$$

are associated with saddle-focus homoclinic loops and are quasi-attractors. The corresponding non-robust double-scroll attractor is shown in Fig. 5.

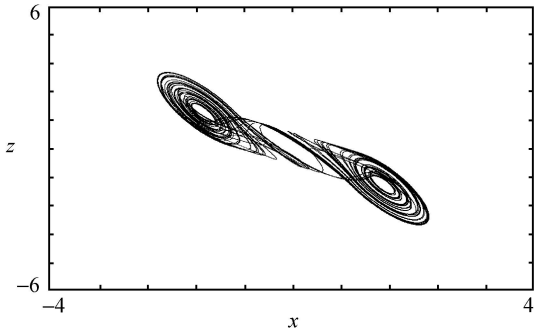

Fig. 5 The non-robust double-scroll attractor obtained from system (20) with $\alpha = 9.35, \beta = 14.79, m_0 = -\dfrac{1}{7}, m_1 = \dfrac{2}{7}$ [45].

4 Discussion

In this paper we discuss the robustness of chaos in the sense that there are no coexisting attractors and no periodic windows in some neighborhood of the parameter space. As we saw, robust chaos occurs in several types of dynamical systems: discrete, continuous-time, autonomous, non-autonomous, smooth, and non-smooth,

with different topological dimensions, and it has been confirmed either analytically, numerically, or experimentally, or a combination of them. On the other hand, there is no robust chaos in the quasi-attractor type because they are structurally unstable.

There are several methods for proving the robustness of chaos in dynamical systems. Some of these methods are collected and summarized in the following:

4.1 Normal form analysis

This method was used essentially (with other techniques) for both 2-D piecewise smooth maps [11, 13, 47, 69, 77] and 3-D continuous-time systems [18]. In both cases, the robustness was proved analytically and confirmed numerically, and in some cases the results were confirmed experimentally.

4.2 Unimodality

Unimodality is an analytic property defined for real functions. This method was used for proving the robustness of chaos in smooth 1-D maps [1–5] with the investigation of their invariant distributions and Lyapunov exponents. This idea came from the analysis of the well-known logistic map.

4.3 Metric entropy

Metric entropy [67] measures the average rate of information loss for a discrete measurable dynamical system. This method was used to prove the robustness of chaos in a one-dimensional map [6] using Kolmogorov-Sinai entropy, and in Ref. [20] the topological entropy was computed in an exact sense for $r = 28$. Other examples can be found in Refs. [53, 54, 70].

4.4 Construction using basis of the robustness or the nonrobustness

If a system is known that has robust chaos, then it is possible to construct another model that has also robust chaos. This method was applied to a hyperbolic-type system [46]. Another example of this method was used to conclude that there is no robust chaos in quasi-attractor-type systems [44, 45].

4.5 Geometric methods

Geometric methods were used to prove the robustness of chaos in the Lorenz system [18, 19, 22, 25–29, 36, 38, 57, 72–75]. These methods employed the so-called geometric model, and a computer-assisted proof was used leading to a rigorous numerical study. Generally, these methods are the most useful for proving chaos or robust chaos in dynamical systems.

4.6 Detecting unstable periodic solutions

This method was used both for discrete and continuous-time systems [20, 43, 49, 72].

4.7 Ergodic theory

Ergodic theory [67] was used to prove the existence of robust chaos in several types of dynamical systems, for example in Ref. [21].

4.8 Weight-space exploration

The method of weight-space exploration is essentially based on two concepts. The first is the concept of running, which is defined as a mapping from the high-dimensional space of the neural network structure (defined by the interconnection weights, the initial conditions, and the nonlinear activation function) to one or two scalar values (called dynamic descriptors) giving the essential information about the dynamic behavior of the network as obtained by running it on a manageable enough large time period. The second concept is called descriptor map. This method was used to search for robust chaos in a discrete CNN such as the example given in Ref. [68].

4.9 Numerical methods

Other than the types of systems mentioned in the above gallery, the regions of parameters space for multiple attractors (regions of fragile chaos), were determined using a relatively large number N of different random initial conditions and looking for cases where the distribution of the average value of the state variable on the attractor is bimodal. Since there is no rigorous test for bimodality, this was done by sorting the N values of the state variable and then dividing them into two equal groups.

The group with the smallest range of the state variable was assumed to represent one of the attractors, and a second attractor was assumed to exist if the largest gap in the values of those in the other group was twice the range of the first group. This method allowed us to see regions of robust chaos (without multiple attractors) as shown in Ref. [68] and in Fig. 6.

4.10 Combination of several methods

In most examples of systems that have robust chaos, it

is easy to see that the proof is a combination of several methods.

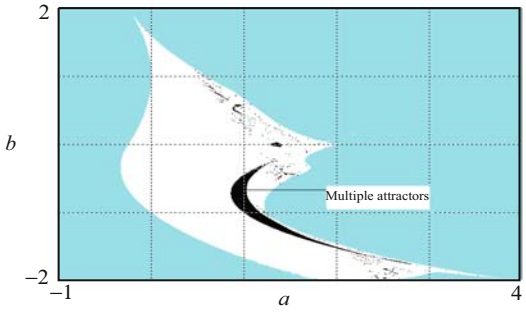

Fig. 6 The regions of *ab*-space for multiple attractors for the map given in Ref. [68].

5 Conclusion

An overview on some issues of common concern related to the robustness of chaos in dynamical systems with several examples in the real world were given and discussed in this paper.

References

1. M. Andrecut and M. K. Ali, Inter. J. Mod. Phys. B, 2001, 15(2): 177
2. M. Andrecut and M. K. Ali, Mod. Phys. Lett. B, 2001, 15(12–13): 391
3. M. Andrecut and M. K. Ali, Europhys. Lett., 2001, 54: 300
4. M. Andrecut and M. K. Ali, Phys. Rev. E, 2001, 64: 025203(R)
5. P. Gabriel, Inter. J. Bifur. Chaos, 2004, 14(7): 2431
6. M. A. Jafarizadeh and S. Behnia, J. Nonlinear. Math. Phys., 2002, 9(1): 26
7. D. Singer, SIAM Journal on Applied Mathematics, 1978, 35(2): 260
8. E. Barreto, B. Hunt, C. Grebogi, and J. A. Yorke, Phys. Rev. Lett., 1997, 78: 4561
9. R. Lozi, Colloque C5, Supplément au n^0 8, 1978, 39: 9
10. M. Hénon, Commun. Math. Phys., 1976, 50: 69
11. B. Robert and C. Robert, Int. J. Control, 2002, 75(16–17): 1356
12. S. Banerjee and C. Grebogi, Phy. Rev. E, 1999, 59(4): 4052
13. S. Banergee, J. A. York, and C. Grebogi, Phys. Rev. Lett., 1998, 80(14): 3049
14. M. A. Hassouneh, E. Habed, and S. Banerjee, Feedback Control of Border Collision Bifurcations in Two-dimensional Discrete-time Systems, ISR Technical Research Report, 2002
15. J. M. Ottino, The Kinematics of Mixing: Stretching, Chaos, and Transport, Cambridge: Cambridge University Press, 1989
16. J. M. Ottino, F. J. Muzzion, M. Tjahjadi, J. G. Franjione, S. C. Jana, and H. A. Kusch, Science, 1992, 257: 754
17. E. N. Lorenz, J. Atmos. Sci., 1963, 20: 130
18. W. Tucker, C. R. Acad. Sci. Paris Ser. I: Math, 1999, 328(12): 1197
19. I. Stewart, Nature, 2000, 406: 948
20. V. Franceschini, C. Giberti, and Z. Zheng, Nonlinearity, 1993, 6: 251
21. M. Majumdar and T. Mitra, Economic Theory, 1994, 4(5): 677
22. C. A. Morales, M. J. Pacifico, and E. R. Pujalls, Annals of Mathematics, 2004, 160(2): 375
23. T. Archibald, Centaurus, 1988, 31(2): 141
24. B. Widrow and M. A. Lehr, 30 Years of Adaptive Neural Networks: Perceptron, Madaline, and Backpropagation, Proc. IEEE, 1990, 78 (9): 1415
25. Z. Galias and P. Zgliczynski, Physica D, 1998, 115: 165
26. J. Guckenheimer, A Strange, Strange Attractor, In: The Hopf Bifurcation and Its Applications, edited by Marsden and McCracken, New York: Springer-Verlag, 1976
27. J. Guckenheimer and R. F. Williams, Publ. Math. IHES, 1979, 50: 307
28. S. P. Hasting and W. C. Troy, Bull. Amer. Math. Soc, 1992, 27: 298
29. K. Mischaikow and M. Mrozek, Bull. Amer. Math. Soc., 1995, 32: 66
30. M. Mukul and T. Mitra, Ricerche Economiche, 1994, 48: 225
31. D. Rand, Math. Proc. Camb. Phil. Soc., 1978, 83: 451
32. C. Robinson, Nonlinearity, 1989, 2: 495
33. M. Rychlik, Ergod. Th. & Dynam. Sys., 1989, 10: 793
34. S. Smale, Math. Intelligencer, 1998, 20: 7
35. C. Sparrow, The Lorenz Equations: Bifurcations, Chaos, and Strange Attractors, New York: Springer-Verlag, 1982
36. W. Tucker, Foundations of Computational Mathematics, 2002, 2(1): 53
37. R. F. Williams, Publ. Math. IHES, 1979, 50: 321
38. V. Araujo, M. J. Pacifico, E. R. Pujals, and M. Viana, preprint, arXiv: math.DS/0511352
39. V. S. Anishchenko and G. I. Strelkova, Attractors of Dynamical Systems, Control of Oscillations and Chaos, 1997. Proc. 1st International Conference, 27–29 Aug. 1997, Vol. 3: 498
40. S. Banerjee and G. C. Verghese (eds.), Nonlinear Phenomena in Power Electronics: Attractors, Bifurcations, Chaos, and Nonlinear Control, USA, New York: IEEE Press, 2001
41. F.-Y. Sun, S.-T. Liu, and Z.-W. Lv, Chinese Physics, 2007, 16(12): 3616
42. U. Vikas and R. Kumar, Chaos, Solitons & Fractals, 2004, 21(5): 1195
43. A. Potapov and M. K. Ali, Phy. Lett. A, 2000, 277(6): 310
44. C. Mira, Inter. J. Bifur. Chaos, 1997, 7(9): 1911
45. L. O. Chua, M. Komuro, and T. Matsumoto, IEEE Transaction in Circuit and System, 1986, CAS-33: 1073
46. S. Kuznetsov and E. Seleznev, Journal of Experimental and

Theoretical Physics, 2006, 102(2): 355
47. P. Kowalczyk, Nonlinearity, 2005, 18: 485
48. R. Dogaru, A. T. Murgan, S. Ortmann, M. G lesner, Searching for Robust Chaos in Discrete Time Neural Networks Using Weight Space Exploration, Proc. ICNN'96, Washington D. C., 2–6 June, 1996
49. B. Henk, E. Konstantinos, and S. Easwar, Nonlinearity, 2008, 21(1): 13
50. E. Kei, I. Takahiro, and T. Akio, IEICE Trans. Fundamentals of Electronics, Communications and Computer Sciences, 1998, E81-A (6): 1223
51. U. S. Bhalla and R. Lyengar, Chaos, 2001, 11: 221
52. R. V. Plykin, Russ. Math. Surv., 2002, 57(6): 1163
53. M. C. Shastry, N. Nagaraj, and P. G. Vaidya, The β-Exponential Map: A Generalization of the Logistic Map, and Its Applications in Generating Pseudo-random Numbers, preprint
54. N. V. Nithin, G. Prabhakar, Bhat, and G. Kishor, Joint Entropy Coding and Encryption Using Robust Chaos, preprint
55. H. Kantz, C. Grebogi, A. Prasad, Y.-C. Lai, and E. Sinde, Phys. Rev. E, 2002, 65: 026209
56. V. S. Anishenko, T. E. Vadivasova, G. I. Strelkova, and A. S. Kopeikin, Discrete Dynamics in Nature and Society, 1998, 2: 249
57. N. E. Klinshpont, E. A. Sataev, and R. V. Plykin, Journal of Physics: Conference Series, 2005, 23: 96
58. R. Yulmetyev, N. Emelyanova, S. Demin, F. Gafarov, P. Hänggi, and D. Yulmetyeva, Fluctuations and Noise in Stochastic Spread of Respiratory Infection Epidemics in Social Networks, Unsolved Problems of Noise and Fluctuations UPoN, 3rd International Conference, 2002: 408
59. T. Dan, Prog. Theor. Phys., Suppl., 2006, 61: 119
60. G. D. Ruxton and P. Rohani, Theoretical Population Biology, 1998, 53(3): 175
61. M. Drutarovsky and P. A. Galajda, Radioengineering, 2007, 16(3): 120
62. J. A. Vano, J. C. Wildenberg, M. B. Anderson, J. K. Noel, and J. C. Sprott, Nonlinearity, 2006, 19(10): 2391
63. H. T. Yau and J. J. Yan, Chaos, Solitons and Fractals, 2004, 19(4): 891
64. B. Adrangi and A. Chatrath, Applied Financial Economics, 2003, 13(4): 245
65. M. Tapan and S. Gerhard, Japanese Economic Review, 1999, 50(4): 470
66. P. Ashwin and A. M. Rucklidge, Physica D, 1998, 122(1): 134
67. I. P. Cornfeld, S. V. Fomin, and Ya G. Sinai, Ergodic Theory, Berlin: Springer-Verlag, 1982
68. Z. Elhadj and J. C. Sprott., Inter. J. Bifur. Chaos, 2008, 18(4), to appear
69. Z. Elhadj and J. C. Sprott., A Unified Piecewise Smooth Chaotic Mapping that Contains the Hénon and the Lozi Systems, submitted
70. O. Alvarez-Llamoza, M. G. Cosenza, and G. A. Ponce, Chaos, Solitons & Fractals, 2008, 36(1): 150
71. A. Priel and I. Kanter, Europhys. Lett., 2000, 51(2): 230
72. V. S. Afraimovich, V. V. Bykov, and L. P. Shil′nikov, Trans. Moscow Math. Soc., 1982, 44: 153
73. B. Hassard, J. Zhang, S. P. Hastings, and W. C. Troy, Appl. Math. Lett., 1994, 7: 79
74. K. Mischaikow and M. Mrozek, Bull. Amer. Math. Soc., 1995, 32(1): 66
75. K. Mischaikow and M. Mrozek, Math. Comp., 1998, 67 (223): 1023
76. Y. Chen and Y. Liu, Up-embeddability of a Graph by Order and Girth, Graphs and Combinatorics, 2007, 23(5): 521
77. S. Banerjee, D. Kastha, S. Das, G. Vivek, and C. Grebogi, Robust Chaos—the Theoretical Formulation and Experimental Evidence, ISCAS, 1999, 5: 293
78. V. Vijayaraghavan and L. Leung Henry, A Robust Chaos Radar for Collision Detection and Vehicular Ranging in Intelligent Transportation Systems, ITSC, 2004: 548
79. S. Shanmugam and H. Leung, A Robust Chaotic Spread Spectrum Inter-vehicle Communication Scheme for ITS, IEEE International Conference on Intelligent Transportation Systems, Shanghai, China, Oct. 2003: 1540
80. M. P. Dafilis, D. T. J. Liley, and P. J. Cadusch, Chaos, 2001, 11(3): 474